AGU PUBLICATIONS

Geophysical Research Letters

RESEARCH LETTER
10.1002/2017GL073138

Key Points:
- Coralline algae yield 342 year reconstruction of Aleutian sea surface temperatures
- Transient decadal-scale variability in the North Pacific Ocean
- Aleutian sea surface temperatures linked to North Pacific cyclone variance

Supporting Information:
- Supporting Information S1
- Data Set S1

Correspondence to:
B. Williams,
bwilliams@kecksci.claremont.edu

Citation:
Williams, B., J. Halfar, K. L. Delong, E. Smith, R. Steneck, P. A. Lebednik, D. E. Jacob, J. Fietzke, and G. W. K. Moore (2017), North Pacific twentieth century decadal-scale variability is unique for the past 342 years, *Geophys. Res. Lett.*, *44*, 3761–3769, doi:10.1002/2017GL073138.

Received 20 FEB 2017
Accepted 27 MAR 2017
Accepted article online 30 MAR 2017
Published online 24 APR 2017

North Pacific twentieth century decadal-scale variability is unique for the past 342 years

B. Williams[1], J. Halfar[2], K. L. Delong[3], E. Smith[4], R. Steneck[5], P. A. Lebednik[6], D. E. Jacob[7], J. Fietzke[8], and G. W. K. Moore[9]

[1]W.M. Science Department, Claremont McKenna College, Pitzer College, Scripps College, Claremont, California, USA, [2]Department of Chemical and Physical Sciences, University of Toronto, Mississauga, Ontario, Canada, [3]Department of Geography and Anthropology, Louisiana State University and A. & M. C., Baton Rouge, Louisiana, USA, [4]Claremont McKenna College, Claremont, California, USA, [5]Darling Marine Center, School of Marine Sciences, University of Maine, Walpole, Maine, USA, [6]LEBCON Environmental Services, Walnut Creek, California, USA, [7]Department of Earth and Planetary Sciences, Macquarie University, Sydney, New South Wales, Australia, [8]GEOMAR, Helmholtz Centre for Ocean Research, Kiel, Germany, [9]Department of Physics, University of Toronto, Toronto, Ontario, Canada

Abstract Reconstructed sea surface temperatures (SSTs) derived from Mg/Ca measurements in nine encrusting coralline algal skeletons from the Aleutian archipelago in the northernmost Pacific Ocean reveal an overall increase in SST from 1665 to 2007. In the Aleutian SST reconstruction, decadal-scale variability is a transient feature present during the 1700s and early 1800s and then fully emerging post-1950. SSTs vary coherently with available instrument records of cyclone variance and vacillate in and out of coherence with multicentennial Pacific Northwest drought reconstructions as a response to SST-driven alterations of storm tracks reaching North America. These results indicate that an influence of decadal-scale variability on the North Pacific storm tracks only became apparent during the midtwentieth century. Furthermore, what has been assumed as natural variability in the North Pacific, based on twentieth century instrumental data, is not consistent with the long-term natural variability evident in reconstructed SSTs predating the anthropogenic influence.

1. Introduction

Decadal-scale variability in North Pacific Ocean seawater temperatures influences atmospheric circulation systems, which in turn influences global precipitation/drought events through alteration of storm tracks and modulation of the El Niño–Southern Oscillation [*Hartmann*, 2015; *Nigam et al.*, 1999; *Wang et al.*, 2014]. Our understanding of this North Pacific variability is drawn from climate model output, instrumental data, and proxy-based reconstructions [*Newman et al.*, 2016]. However, current models underestimate tropical influence on Pacific decadal variability in the Northern Hemisphere relative to observations based on the instrument data [*Newman et al.*, 2016]. Whether our understanding of model parameters, quality of instrumental data, or a combination of both causes this inconsistency is unknown. The instrumental data include interpolated gridded sea surface temperature (SST) data products that use the International Comprehensive Ocean-Atmosphere Data Set (ICOADS) [*Worley et al.*, 2005] as the SST source. Increasing uncertainty characterizes these data sets further back in time due to the limited duration and spatial coverage of the ICOADS observations [*Deser et al.*, 2010]. These data products indicate coherent spatial and temporal climate variability for much of the twentieth century. Yet increasing anthropogenic emissions of greenhouse gases to the atmosphere characterize the period with best data coverage, and global temperatures during this period are exceeding the estimates of natural variability [*Bindoff et al.*, 2013]. Therefore, anthropogenic climate change may be influencing our current understanding of the drivers of northern North Pacific climate variability and its interactions with other climate elements. Data sets that extend further back in time are necessary to understand the role of "natural" decadal-scale variability on climate to place current climatic changes in a long-term context.

One source of proxy-based climate records extending into the past are the tree ring-based reconstructions in the areas adjacent to the North Pacific [*Biondi et al.*, 2001; *D'Arrigo and Wilson*, 2006; *D'Arrigo et al.*, 2001; *Gedalof and Smith*, 2001; *MacDonald and Case*, 2005]; however, these reconstructions do not vary coherently because of increasing proxy uncertainty and/or changes in the spatial pattern of past climate variability [*Kipfmueller et al.*, 2012]. As such, there is little agreement among these available records of decadal-scale

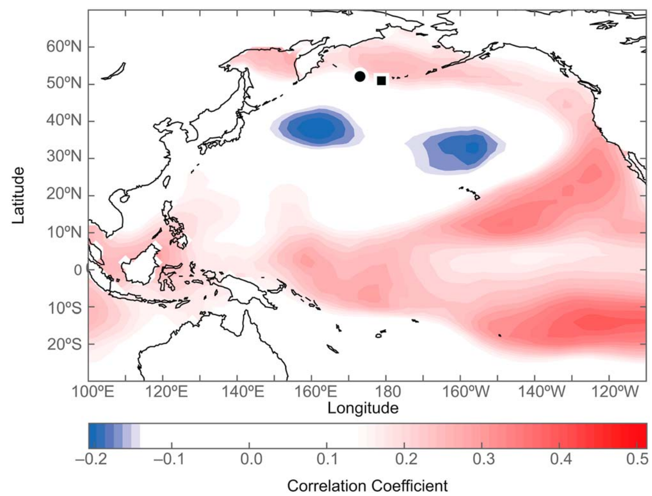

Figure 1. Correlation map of SST anomalies from algal SST with ERSST [*Smith et al.*, 2008] for the years 1960–2003 is similar to the spatial SST pattern representing the Pacific Decadal Oscillation [*Mantua et al.*, 1997]. SST anomalies were determined using the monthly climatology for 1971–2000 and low pass filtered to 36 months. Attu and Amchitka Islands marked by circle and square, respectively. Correlations shown are significant (5%) adjusted for degrees of freedom.

behavior in the climate of the North Pacific prior to the twentieth century [*Kipfmueller et al.*, 2012; *Newman et al.*, 2016]. Furthermore, there are no annually resolved reconstructions of in situ SSTs prior to 1949 from the northern boundary of the Pacific (i.e., the Aleutian archipelago). This means that our understanding of SST variability in the Aleutian archipelago relies on land-based proxies distant to the Aleutians, e.g., tree rings and speleothems [*D'Arrigo et al.*, 1999; *McCabe-Glynn et al.*, 2013], whose relationships may change through time [*D'Arrigo et al.*, 2008]. These changing relationships such as potential modification of the North Pacific storm track may be occurring, particularly over the past several decades [*Salathe*, 2006], as increasing concentrations of atmospheric greenhouse gases play a larger role in global climate [*Bindoff et al.*, 2013].

To quantify climate variability in the northern North Pacific and the mechanisms driving this variability, we reconstructed 342 years of proxy-based SSTs extracted from the skeletons of encrusting coralline algae. To do this, multiple specimens of the long-lived coralline alga *Clathromorphum nereostratum* Lebednik were collected from two islands in the central western portion of the Aleutian archipelago (Figure 1). *C. nereostratum* is prolific in near-surface rocky seafloor environments in the Aleutian archipelago with reported longevity of 850 years [*Adey et al.*, 2013; *Halfar et al.*, 2007]. Winter decreases in temperature and insolation, sometimes combined with the start of reproduction, reduces calcification in this alga. This reduction in calcification produces clear annual growth increments [*Adey*, 1965; *Moberly*, 1968]. Magnesium content in the alga's high-Mg calcite skeleton varies from ~6 to 14 mol % $MgCO_3$ in response to ambient temperature at the time of formation [*Hetzinger et al.*, 2009]. Thus, Mg/Ca measurements across the skeleton of the alga produce subannually resolved records of past seawater temperatures. This work builds upon our calibration and verification study that assessed skill and error in reconstructing past SST from this alga [*Williams et al.*, 2014]. Here we apply this calibration to generate a replicated in situ SST reconstruction. From this SST reconstruction, we interpret drivers of decadal-scale and long-term variability present in the northernmost North Pacific.

2. Methods and Data

Nine *C. nereostratum* specimens were collected on the seafloor by scuba divers in the northeast and the southeast coasts of Attu Island and to the northeast of Amchitka Island in the Aleutian archipelago (Figure 1 and supporting information Table S1 and Figure S1a). This alga provides significant substrate, refuge, and food to a variety of invertebrate organisms in the Aleutians, resulting in a robust shallow seafloor community on par with the microalgal habitats [*Chenelot et al.*, 2011]. Wild specimens from Attu and Amchitka Islands were obtained during expeditions in August 2004 and June 2008, and from a museum collection containing samples collected in 1969 (Herbarium of University of British Columbia, Vancouver). Approximately 1 cm thick cross sections of each specimen were made cutting parallel to the direction of growth. Sections were polished and imaged at 50X magnification using an Olympus reflected light microscope (VS-BX) with automated sampling stage and imaging system. The produced images were stitched together using geo.TS software to form a single high-resolution photomosaic of each section (supporting information Figure S1b). Two relatively parallel digital paths along the axis of maximum growth visible on the photomosaics for each specimen were selected for Mg/Ca analysis. Skeletal ^{24}Mg and ^{43}Ca values were measured using an Agilent 7500ce quadrupole inductively coupled plasma–mass spectrometry (ICP-MS) coupled to a New Wave Research UP-213 laser ablation system (neodymium: yttrium/aluminum/garnet, Nd:YAG laser) with helium as carrier gas at the Department of Geosciences, Johannes Gutenberg-Universität, Mainz, Germany. NISTSRM610 (U.S. National Institute of Standard and Technology Standard Reference Material) glass was used as the external standard. Samples were ablated in continuous lines after preablation of the surface. The standard deviations of recurrent analyses of the NISTSRM610 standard every 30 min were always within 10%, indicating that instrumental drift was insignificant. The relative standard deviation for recurrent analysis of NISTSRM610 was ≤1%.

We used annual growth increments identified in the high-resolution photomosaic images combined with annual maxima and minima in the Mg/Ca values (supporting information Figure S1c) to create chronologies for each of the specimens with continuous growth (supporting information Figure S2). The three specimens 08-01-06-G1, 08-01-07-G2-1, and 08-01-07_G2-3b were collected live, yet disconformities in the skeleton representing a disruption of growth were evident in the skeleton of these specimens. Therefore, we used U-Th dating [*Fietzke et al.*, 2005] to develop floating chronologies for the skeleton formed below the growth disconformities (supporting information Table S2 and Figure S2). The U^{234}/U^{238} and U^{238}/Th^{232} ratios in the skeleton below the growth disconformities in these specimens was similar to that in the specimen AT11-4 that did not have a growth disconformity. This indicates that the algal skeleton is a closed system, and there is no diagenetic overprinting preventing the use of this dating technique in these specimens. To refine the U-Th-determined floating chronology of the skeleton formed below a growth disconformity, we used cross correlation (or crossdating) of the Mg/Ca records (supporting information Tables S1 and S2) as follows. Growth increments around each U-Th date were assigned a year by counting outward from the skeletal location of the U-Th-dated sample. This preliminary chronology was applied to the Mg/Ca values. The chronology was then fine-tuned by optimizing the cross correlation with the master record derived by averaging the Mg/Ca values from all the specimens with continuous growth (no growth disconformities) at both islands. The dating optimization was done by shifting the U-Th-derived chronologies forward and backward in time within U-Th dating uncertainty (2σ) to obtain the highest correlation with the master record. All final adjustments were within the 2σ uncertainty of the U-Th ages (supporting information Table S2). This crossdating approach is comparable to that used in other fields of sclerochronology [*Butler et al.*, 2009; *Cobb et al.*, 2013; *DeLong et al.*, 2012, 2014].

The measured Mg/Ca records for each specimen were converted to absolute SST (supporting information Figure S3) using verified transfer functions developed in *Williams et al*. [2014]. These transfer functions used the maximum and minimum monthly Mg/Ca values. This gives equal weight to the shorter 3 month summer (temperatures above 8°C) as the longer 5 month winter (temperatures below 4°C) characterizing the central western Aleutian archipelago. Here we used all available Mg/Ca values to determine absolute SST. To reduce the impact of subannual dating uncertainty, we either filtered monthly data interpolated from the raw data using Analyseries software [*Paillard et al.*, 1996] with a 36 month low-pass filter or annually averaged the reconstructed SSTs. These reconstructed SSTs were consistently higher (average 0.47°C for the interval from 1971 to 2000) than expected from annual average temperatures determined from the gridded SST data products ERSST [*Smith et al.*, 2008] and Hadley Centre Sea Ice and SST version 1.1 (HadISST) [*Rayner et al.*, 2003] for the area of this study. We applied a −0.47°C offset to the entire SST reconstruction for comparison to those data products to account for differences between the data products SST and that experienced by the algae and the seasonal bias in the calibration.

Agreement between the reconstructed interannual SSTs for the two islands ($r = 0.53$, $p < 0.0001$, degrees of freedom (d.f.) = 109, for the overlapping period 1838–2003 and 36 month low pass filtered) supported averaging the two island-based reconstructions together to create a unified Aleutian SST reconstruction (Figure 2c and supporting information Figure S3). This master reconstruction of Aleutian SSTs spanned the full timeframe from 1665 to 2007 (Figure 2c). The d.f. for all correlation analysis were calculated using the Runs test [*Draper and Smith*, 1998] to account for autocorrelation that tends to inflate significant levels. The SST reconstruction significantly correlated with SST from ERSST ($r = 0.47$, $p < 0.005$, d.f. = 31) and HadISST ($r = 0.63$, $p < 0.001$, d.f. = 31) for January 1960 to June 2007 (both 36 month low pass filtered). For comparison, grid-level SSTs from ERSST and HadISST also significantly correlate ($r = 0.85$, $p < 0.0005$, d.f. = 36). Here the validation tests comparing the different SSTs used the interval of 1960 to 2007 because the number of

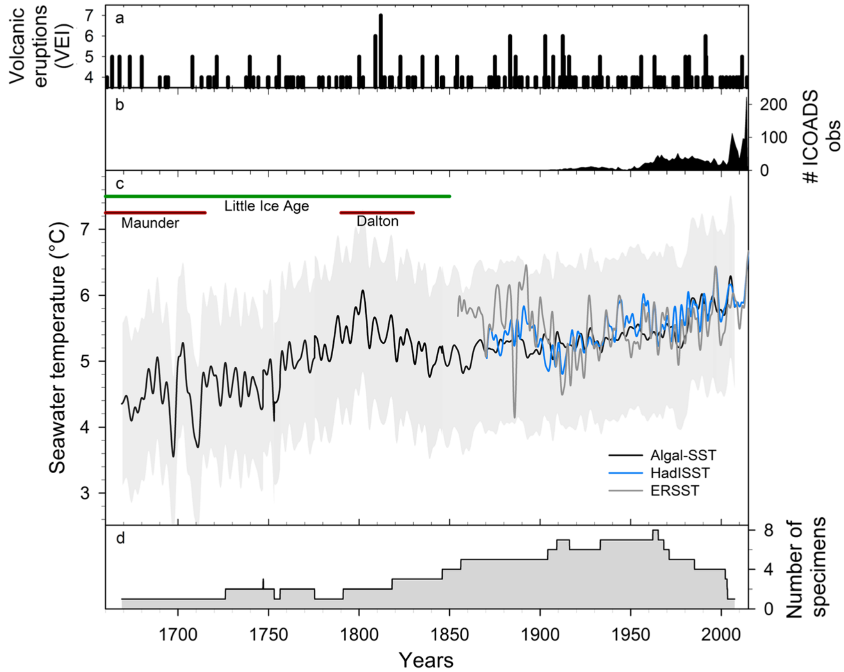

Figure 2. Comparison of the alga SST reconstruction with volcanic and solar variability. (a) Volcanic eruptions with a Volcanic Explosivity Index (VEI) ≥ 4 [*Simkin and Siebert*, 1994]. (b) Number (#) of observations per year contributing to ICOADS [*Worley et al.*, 2005] for the grid area (50–54°N,170–184°E) that includes Attu and Amchitka Islands. (c) Reconstructed SSTs (black line) smoothed with a 36 month low-pass filter with the error of reconstruction (shaded area; 1 standard deviation) based on (d) the number of specimens for each month compiled to generate the reconstruction. The gridded data products HadISST (blue dashed line) [*Rayner et al.*, 2003] and ERSST (grey line) [*Smith et al.*, 2008] post-1900 for the grid area 49–55°N, 171–181°E enclosing our study site are shown for comparison and are similarly smoothed. All these records (gridded and reconstructed) start to diverge as the number of records in the ICOADS decreases. Timing of the Maunder and Dalton solar minimums (red) are noted along with the Little Ice Age (green).

observations in ICOADS that contributes to the ERRST and HadISST data products is greatly reduced before 1960 in our study area and is thus less reliable (Figure 2b).

We determined the monthly anomalies for the SST reconstruction with respect to the 30 year interval 1971 to 2000. For comparison with annual records of other climate variability, we averaged the monthly reconstructed SST anomalies for each calendar year. The error of the reconstruction was assessed for escalating scales from a single specimen to four specimens by calculating the standard error of regression for the calibration interval (1960–2007) [*Williams et al.*, 2014]. Four was the largest number of algal records available post-1960 for the calibration interval for error assessments. Yet at times the reconstruction combined up to eight specimens contributing to the unified reconstruction (Figure 2c). Thus, the actual error of the SST reconstruction is overestimated for these intervals. We used frequency analysis methods to assess significant (5%) periodicities of variability in the reconstructed SSTs. We perform this analysis twice, once for the interval post-1850 and once for the entire record. This prevents the larger fluctuations present in the earlier part of the SST reconstruction (e.g., prior to 1725) generated from only one specimen from swamping out the muted variability later in the reconstruction (e.g., post-1850) generated from averaging SSTs derived from multiple specimens together. We assessed significance (5%) of secular changes in the monthly SST reconstruction using Monte Carlo simulation with 10,000 realizations of the SST reconstruction. The simulation was allowed to vary within the reconstruction uncertainty (Gaussian distribution) determined for each month based on the number of specimens. This method included nonclimatic variability in our significance testing.

3. Interpretation of Aleutian SST Time Series

3.1. Verification of Proxy Archive

Correlation analysis of the 36 month low-pass-filtered reconstructed SSTs with the similarly filtered gridded ERSST data product reveals a spatial pattern (Figure 1) similar to the Pacific Decadal Oscillation (PDO), the primary mode of North Pacific SST variability [*Newman et al.*, 2016]. The reconstructed SSTs significantly correlate (r = 0.2 to 0.4) with ERSST in the Bering Sea, along the Aleutian archipelago, northeastern Gulf of Alaska, and into the subtropical and tropical eastern Pacific and negatively correlate ($r = -0.2$) in the central North Pacific Ocean. This spatial correlation pattern is consistent with that found using annually resolved National Centers for Environmental Prediction Optimally Interpolated SST (NCEP OISST) [*Reynolds et al.*, 2002] selected for the grid encompassing Attu and Amchitka Islands with ERSST (supporting information Figure S4) with one exception: the reconstructed SSTs significantly correlate with Southern Hemisphere subtropical eastern Pacific gridded ERSSTs while the NCEP OISST do not. OISST includes satellite-derived SST with better spatial coverage than ERSST thus may better reflect actual Pacific Ocean coherence; however, OISST is temporally limited to 1981 to present. For this reason, we used ERSST for calibration of the algal reconstruction for the longer time interval.

3.2. Decadal-Scale Variability

The reconstructed SSTs significantly correlate with the PDO time series [*Mantua et al.*, 1997] post-1945 (r = 0.39, p = 0.0017, n = 62 for annual averages) (Figures 3b and 3e). The short negative deviation in Aleutian SSTs marking the 1976–1977 PDO transition is consistent with PDO instrumental records and reconstructions derived from tree ring climate archives [*Gedalof and Smith*, 2001]. The 1922 and 1945 PDO shifts are not evident in Aleutian SSTs indicating a change in climate of the Aleutians after the 1945 PDO shift that aligns the Aleutian climate with the broader North Pacific climate. The absence of a consistent temporal relationship between Aleutian SSTs and the PDO is supported by the absence of covariability of the SST reconstruction with the tree ring-derived PDO reconstruction on longer timescales (supporting information Figure S6a) [*MacDonald and Case*, 2005]. Furthermore, wavelet analysis of the reconstructed SST anomalies post-1850 reveals the emergence of significant decadal-to-bidecadal variability only since 1950 (Figure 3a). Variability on ~30 to 45 year timescales is persistent through the first half of the record until the 1820s (Figure 4) and returns as part of the bidecadal variability post-1945 (Figure 3a). The reduced decadal-to-bidecadal variability from 1840 to 1930 is consistent with previous studies finding anomalous variability in the North Pacific region during this time period [*Gedalof and Smith*, 2001]. In contrast to the transient decadal-to-bidecadal scale variability, the reconstructed SST anomalies vary on $>$50 year timescales (Figures 3a and 4a). This is consistent with North American tree ring records indicating coherence in the North Pacific region with North America climate variability [*Minobe*, 1997].

Here we find that Aleutian SSTs significantly negatively correlate with the North Pacific Index (NPI) such that warmer temperatures occur when the Aleutian Low is stronger ($r = -0.21$, p = 0.027, n = 109 for annual averages). However, the relationship is not robust if the secular long-term trends are removed ($r = -0.05$, p = 0.60, n = 109, detrended using a linear fit over the duration of the entire record). Thus, the correlation is largely driven by the century-long warming trend in the reconstructed SSTs corresponding to the decreasing NPI since 1899. Furthermore, the reconstructed SSTs did not significantly vary with the amount of light reaching the shallow seafloor in the archipelago, which was determined through measurements of growth rates in *C. nereostratum* [*Halfar et al.*, 2011]. In the Aleutians, the shallow seafloor light dynamics reflect changes in the long-term strength of the Aleutian Low [*Halfar et al.*, 2011]. The absence of a relationship between reconstructed SSTs and the strength of the Aleutian Low is consistent with findings using reanalysis data set post-1950 that the strength of the Aleutian Low does not drive regional winter temperatures [*Rodionov et al.*, 2007]. In contrast, the location of the Aleutian Low impacts storm tracks and winter temperatures in the Bering Sea [*Rodionov et al.*, 2007]. Testing for the effect of variance in cyclone activity on the Aleutian climate, we compared the SST reconstruction to cyclone variability [*Blackmon et al.*, 1977]. We find that the SST reconstruction significantly correlates with the cyclone variance proxies (r = 0.41, p = 0.0001, n = 86 for ERA-20C [*Poli et al.*, 2015] and r = 0.37, p = 0.0005, n = 86 for 20CRv2 [*Compo et al.*, 2011]) for the region inclusive of the western Aleutian archipelago from 1920 to 2005 with a 2 year lead in SSTs (Figures 3b and 3d). The year 1920 was selected because surface pressure measurements from the northernmost Pacific region start in the 1920s. Maximum covariate analysis of the 20CRv2 and HadISST data set indicates that a PDO-like pattern of SST anomalies induced a positive storm track anomaly along 50°N with a 2 year lead in the temperature anomalies [*Gan and Wu*, 2013], consistent with our results. Because cyclones passing through the Aleutians have been diverted from their primary west-to-east storm track, they do not reach the northwest coast of North America [*Rodionov et al.*, 2007]. Thus, the track that these cyclones follow

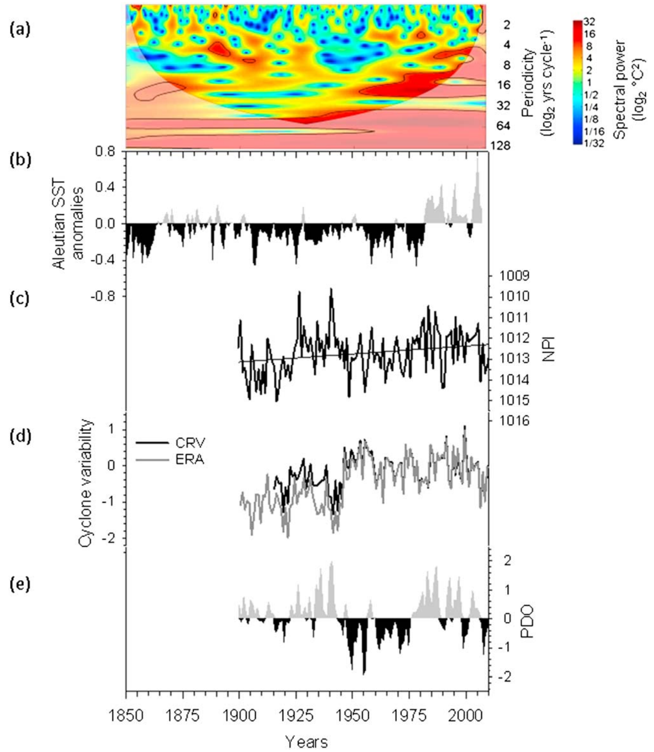

Figure 3. Spectral analysis of the alga SST reconstruction with climate indices post-1850. (a) Wavelet spectrum (Morlet mother wavelet) of reconstructed monthly SST anomalies linearly detrended with thin black contour lines enclosing time-periodicity regions with significant ($p \leq 0.05$) concentrations of spectral power tested assuming a first-order autoregressive (AR(1)) model and shaded area is the cone of influence [*Grinsted et al.*, 2004; *Torrence and Compo*, 1998]. (b) Detrended SST reconstruction shown as annually averaged anomalies. (c) North Pacific Index (NPI) [*Trenberth and Hurrell*, 1994], plotted on an inverted *y* axis. Trend line represents linear trend calculated for the entire index period. (d) Annual averages of the monthly mean (3–10 day band-pass-filtered variance) sea level pressure field in the North Pacific, which is a proxy for cyclone variability [*Blackmon et al.*, 1977], derived from the European Centre for Medium-Range Weather Forecast's ERA-20C (ERA) [*Poli et al.*, 2015] and National Oceanic and Atmospheric Administration's twentieth Century Reanalysis version 2 (20CRv2) (CRV) [*Compo et al.*, 2011]. (e) Pacific Decadal Oscillation (PDO) [*Mantua et al.*, 1997].

influences precipitation in the Pacific Northwest. Comparison of Aleutian SSTs with a multicentennial reconstruction of the Palmer Drought Severity Index [*Cook and Krusic*, 2004] for locations in the Pacific Northwest indicates variable periods of coherence on the interannual to decadal timescales (supporting information Figure S5b). This result indicates a relationship between the Aleutian SST reconstruction and storm-driven drought conditions in the Pacific Northwest via northwest alteration of storm tracks.

3.3. Long-Term SST Variability

Reconstructed SSTs significantly warmed (1.1 ± 0.30°C (1σ) determined using Monte Carlo simulation) from 1660s to 1800 (rate of change: 0.008 ± 0.002°C/yr (1σ)), followed by a significant cooling of 0.8 ± 0.04°C (1σ) until 1840 (rate of change: 0.02 ± 0.001°C/yr (1σ)), then a significant warming of 0.8 ± 0.16°C (1σ) from 1860 until the end of reconstruction in 2007 (rate of change: 0.005 ± 0.001°C/yr (1σ)) (Figure 2c). Since the earliest warming interval has larger uncertainty resulting from fewer available algal specimens (Figure 2d), the SST increase in this interval is less constrained than the warming in the twentieth century; however, this warming is significant as assessed by reconstruction errors using Monte Carlo simulation. The warming trend post-1850s in the SST reconstruction (0.8 ± 0.16°C, 1σ) is consistent with global mean warming of 0.85 ± 0.21°C (1σ) from 1880 to 2012 (Figures 4b and 4c), attributed largely to anthropogenic causes [*Bindoff et al.*, 2013; *Hartmann et al.*, 2013]. In contrast, the Northern Hemisphere was broadly cooler during the Little Ice Age (~1400–1850) (Figure 4c), which is largely ascribed to decreased solar irradiance and increased volcanic forcing [*Mann et al.*, 2009]. Therefore, here we test for the influence of solar and volcanic variability on the secular changes in the reconstructed SSTs.

Multi-Taper Method (MTM) spectral analysis [*Ghil et al.*, 2002] of the Aleutian reconstructed SSTs finds a significant periodicity at 11 years (supporting information Figure S5a), which is consistent with sunspot variability in solar irradiance [*Lean*, 2000]. Yet the strength of 11 year periodicity is not a persistent feature of the SST reconstruction; rather, it is a transient feature in the record from 1675 to 1830 (Figure 4a). In fact, the SST reconstruction significantly covaried with a reconstruction of solar irradiance [*Lean*, 2000] on the 11 year periodicity only from ~1745 to 1825 (supporting information Figure S4b). In addition, the reconstructed SSTs were cool during the period of lower than usual solar irradiance called the Maunder minimum (1645–1715) but then warmed and cooled during the Dalton minimum (1795–1830), a second period of reduced solar irradiance (Figure 2c). This indicates that solar irradiance is not the primary factor influencing

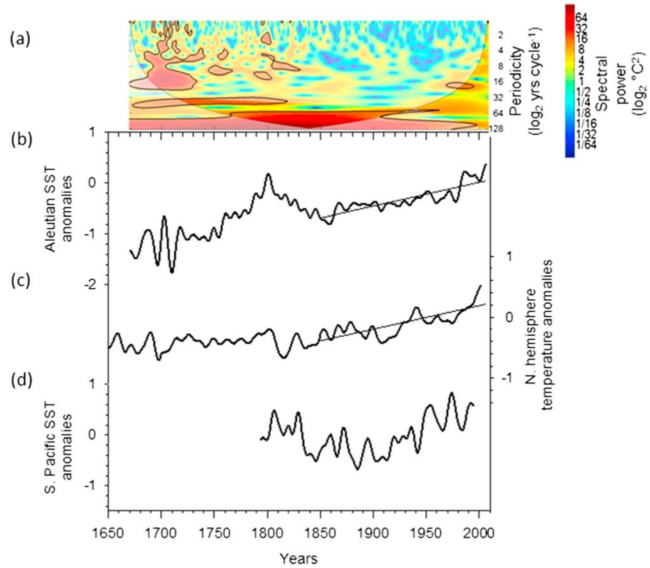

Figure 4. Spectral analysis of the alga SST reconstruction with climate indices from 1665 to 2003. (a) Wavelet spectrum (Morlet mother wavelet) of reconstructed monthly SST anomalies linearly detrended with thin black contour lines enclosing time-periodicity regions with significant ($p \leq 0.05$) concentrations of spectral power tested assuming a first-order autoregressive (AR(1)) model [*Grinsted et al.*, 2004; *Torrence and Compo*, 1998]. Shaded area is the cone of influence for which the results are interpreted with caution due to edge effects that result from zero padding of the time series. (b) Alga SST anomalies compared to (c) anomalies of a Northern Hemisphere temperature reconstruction [*Mann et al.*, 2009], and (d) anomalies of a South Pacific SST reconstruction [*Linsley et al.*, 2015]. Time series in Figures 4b–4d were low pass filtered to decadal resolution. Trend line in Figures 4b and 4c represent linear trend calculated for post-1850 temperatures.

Aleutian SSTs at this periodicity. Comparison of the reconstructed SSTs with volcanic activity using eruptions with the Volcanic Explosivity Index [*Simkin and Siebert*, 1994] of four or higher indicates volcanic activity corresponding with the start of decreasing SSTs in the early 1800s (Figures 2a and 2c). No other relationship exists between volcanic activity and the reconstructed SSTs. The influence of individual volcanic events may be within the error of the calibrated reconstruction or hidden by 36 month filtering of the SST reconstruction and thus is not discernable at this resolution. The Dalton solar minimum and increased volcanic activity in the early 1800s could explain the decreasing SSTs from 1800 to 1850; however, the warming in the late 1700s preceding the cooling (Figure 4c) is not present in the broader Northern Hemisphere multiple-proxy temperature reconstruction [*Mann et al.*, 2009] or the regional eastern tropical multiproxy SST reconstruction [*Tierney et al.*, 2015]. This documented warmth in the North Pacific coincides with a warm period (above average temperatures, ~1800–1810) in the South Pacific recorded in a coral-derived SST reconstruction from Fiji, Tonga, Rarotonga, and New Caledonia caused by unknown forcings [*Linsley et al.*, 2015] (Figure 4d). These coinciding warm periods in the Pacific supports an oceanic role in the late 1700s/early 1800s of Aleutian SST warmth. Yet concurrent above average temperatures in the Aleutians and the tropical South Pacific in the early 1800s are unexpected because these regions are in opposite phasing of the Interdecadal Pacific Oscillation, the primary mode of SST anomalies in the Pacific [*Henley et al.*, 2015]. Therefore, this may reflect a teleconnection between of the South Pacific Decadal Oscillation or Southern Hemisphere Decadal Oscillation [*Hsu and Chen*, 2011; *Shakun and Shaman*, 2009] with the Aleutian Islands. This teleconnection would support a potential role of the tropics in northern North Pacific variability. Finally, the warming trend post-1850s in the SST reconstruction is consistent with an anthropogenic forcing of the larger Northern Hemisphere temperatures. Therefore, these data suggest a complex combination of solar irradiance, volcanic activity, internal ocean dynamics, and external anthropogenic forcing explain the variability in Aleutian SSTs for the past 342 years.

4. Conclusions

Based on the reconstruction of SST, decadal variability is absent in the first half of the twentieth century in the northern North Pacific, only emerging post-1950. Considering the significant influence of decadal-scale variability on global climate, and efforts to understand how this decadal-scale variability may continue evolving as anthropogenic changes to climate occur, it is important to recognize that the last half of the twentieth century exhibits climatic conditions not evident in the period prior to an anthropogenic influence. Thus, studies based on post-1950 instrumental records (e.g., for climate model validation and to determine mechanisms driving climate variability and related teleconnections to distant locations) may not be demonstrably relevant to understanding long-term regional climate conditions.

Acknowledgments

We thank two anonymous reviewers for their comments that helped to improve this manuscript. J.H. acknowledges support from National Sciences and Engineering Research Council of Canada Discovery and Ship Time Grants. The Mg/Ca data used to generate the sea surface temperature reconstruction will be archived at the National Oceanic and Atmospheric Administration's National Centers for Environmental Information upon publication of this article. These data are also available from the authors upon request.

References

Adey, W. (1965), The genus *Clathromorphum* (*Corallinaceae*) in the Gulf of Maine, *Hydrobiologia*, *26*(3–4), 539–573.

Adey, W., J. Halfar, and B. Williams (2013), Biological, physiological and ecological factors controlling high magnesium carbonate formation and producing a precision Arctic/Subarctic marine climate archive: The coralline genus *Clathromorphum* Foslie emend Adey, *Smithson. Contrib. Mar. Sci.*, *40*, 1–48.

Bindoff, N., et al. (2013), Detection and attribution of climate change: From global to regional, in *Climate Change 2013: The Physical Science Basis. Contribution of Working Group I to the Fifth Assessment Report of the Intergovernmental Panel on Climate Change*, edited by T. Stocker et al., Cambridge Univ. Press, Cambridge, U. K., and New York.

Biondi, F., A. Gershunov, and D. Cayan (2001), North Pacific decadal climate variability since 1661, *J. Clim.*, *14*, 5–10, doi:10.1175/1520-0442(2001)1014<0005:NPDCVS>1172.1170.CO;1172.

Blackmon, M., J. Wallace, N.-C. Lau, and S. Mullen (1977), An observational study of the northern hemisphere wintertime circulation, *J. Atmos. Sci.*, *34*(7), 1040–1053, doi:10.1175/1520-0469(1977)1034<1040:AOSOTN>1042.1040.CO;1042.

Butler, P., C. Richardson, J. Scourse, R. Witbaard, B. Schöne, N. Fraser, A. Wanamaker Jr., C. Bryant, I. Harris, and I. Robertson (2009), Accurate increment identification and the spatial extent of the common signal in five *Arctica islandica* chronologies from the Fladen ground, northern North Sea, *Paleoceanography*, *24*, PA2210, doi:10.1029/2008PA001715.

Chenelot, H., S. Jewett, and M. Hobert (2011), Macrobenthos of the nearshore Aleutian archipelago, with emphasis on invertebrates associated with *Clathromorphum nereostratum* (*Rhodophyta*, *Corallinaceae*), *Mar. Biodivers.*, *41*, 413–424, doi:10.1007/s12526-12010-10071-y.

Cobb, K., N. Westphal, H. Sayani, J. Watson, E. Di Lorenzo, H. Cheng, R. Edwards, and C. Charles (2013), Highly variable El Niño–Southern Oscillation throughout the Holocene, *Science*, *339*(6115), 67–70, doi:10.1126/science.1228246.

Compo, G., et al. (2011), The twentieth century reanalysis project, *Q. J. R. Meteorol. Soc.*, *137*, 1–28, doi:10.1002/qj.1776.

Cook, E., and P. Krusic (2004) *The North American Drought Atlas*, Lamont-Doherty Earth Observatory and the National Science Foundation.

D'Arrigo, R., and R. Wilson (2006), On the Asian expression of the PDO, *Int. J. Climatol.*, *26*, 1607–1617, doi:10.1002/joc.1326.

D'Arrigo, R., R. Villalba, and G. Wiles (2001), Tree-ring estimates of Pacific decadal climate variability, *Clim. Dyn.*, *18*, 219–224, doi:10.1007/s003820100177.

D'Arrigo, R., G. Wiles, D. Jacob, and R. Villalba (1999), North Pacific sea surface temperature: Past variations inferred from tree rings, *Geophys. Res. Lett.*, *26*(17), 2757–2760, doi:10.1029/1999GL900504.

D'Arrigo, R., R. Wilson, B. Liepert, and P. Cherubini (2008), On the "Divergence Problem" in northern forests: A review of the tree-ring evidence and possible causes, *Global Planet. Change*, *60*, 289–305, doi:10.1016/j.gloplacha.2007.1003.1004.

DeLong, K., T. Quinn, F. Taylor, K. Lin, and C.-C. Shen (2012), Sea surface temperature variability in the southwest tropical Pacific since AD 1649, *Nat. Clim. Change*, *2*, 799–804, doi:10.1038/nclimate1583.

DeLong, K., J. Flannery, R. Poore, T. Quinn, C. Maupin, K. Lin, and C.-C. Shen (2014), A reconstruction of sea surface temperature variability in the southeastern Gulf of Mexico from 1734 to 2008 CE using cross-dated Sr/Ca records from the coral *Siderastrea siderea*, *Paleoceanography*, *29*, 403–422, doi:10.1002/2013PA002524.

Deser, C., M. Alexander, S.-P. Xie, and A. Phillips (2010), Sea surface temperature variability: Patterns and mechanisms, *Annu. Rev. Mar. Sci.*, *2*, 115–143, doi:10.1146/annurev-marine-120408-151453.

Draper, N., and H. Smith (1998) *Applied Regression Analysis*, 3rd ed., Wiley-Interscience, New York.

Fietzke, J., V. Liebetrau, A. Eisenhauer, and C. Dullo (2005), Determination of uranium isotope ratios by multi-static MIC-ICP-MS: Method and implementation for precise U- and Th-series isotope measurements, *J. Anal. At. Spectrom.*, *20*, 395–401.

Gan, B., and L. Wu (2013), Seasonal and long-term coupling between wintertime storm tracks and sea surface temperature in the North Pacific, *J. Clim.*, *26*(6), 6123–6136, doi:10.1175/JCLI-D-6112-00724.00721.

Gedalof, Z., and D. Smith (2001), Interdecadal climate variability and regime-scale shifts in Pacific North America, *Geophys. Res. Lett.*, *28*(8), 1515–1518, doi:10.1029/2000GL011779.

Ghil, M., et al. (2002), Advanced spectral methods for climatic time series, *Rev. Geophys.*, *40*(1), 1–41, doi:10.1029/2001RG000092.

Grinsted, A., J. Moore, and S. Jevrejeva (2004), Application of the cross wavelet transform and wavelet coherence to geophysical time series, *Nonlinear Process. Geophys.*, *11*, 561–566.

Halfar, J., R. Steneck, B. Schone, G. Moore, M. Joachimski, A. Kronz, J. Fietzke, and J. Estes (2007), Coralline alga reveals first marine record of subarctic North Pacific climate change, *Geophys. Res. Lett.*, *34*, L07702, doi:10.01029/02006GL028811.

Halfar, J., B. Williams, S. Hetzinger, R. Steneck, P. Lebednik, C. Winsborough, A. Omar, P. Chan, and A. Wanamaker Jr. (2011), 225 years of Bering Sea climate and ecosystem dynamics revealed by coralline algal growth-increment widths, *Geology*, *39*, 579–582, doi:10.1130/G31996.31991.

Hartmann, D. (2015), Pacific sea surface temperature and the winter of 2014, *Geophys. Res. Lett.*, *42*, 1894–1902, doi:10.1002/2015GL063083.

Hartmann, D., et al. (2013), Observations: Atmosphere and surface, in *Climate Change 2013: The Physical Science Basis. Contribution of Working Group I to the Fifth Assessment Report of the Intergovernmental Panel on Climate Change*, edited by T. Stocker et al., Cambridge Univ. Press, Cambridge, U. K., and New York.

Henley, B., J. Gergis, D. Karoly, S. Power, J. Kennedy, and C. Folland (2015), A tripole index for the Interdecadal Pacific Oscillation, *Clim. Dyn.*, *45*(11), 3077–3090, doi:10.1007/s00382-00015-02525-00381.

Hetzinger, S., J. Halfar, A. Kronz, R. Steneck, W. Adey, P. Lebednik, and B. Schöne (2009), High-resolution Mg/Ca ratios in a coralline red alga as a proxy for Bering Sea temperature variations from 1902 to 1967, *Palaios*, *24*, 406–412, doi:10.2110/palo.2008.p2108-2116r.

Hsu, H.-H., and Y.-L. Chen (2011), Decadal to bi-decadal rainfall variation in the western Pacific: A footprint of South Pacific decadal variability?, *Geophys. Res. Lett.*, *38*, L03703, doi:10.1029/2010GL046278.

Kipfmueller, K., E. Larson, and S. St. George (2012), Does proxy uncertainty affect the relations inferred between the Pacific Decadal Oscillation and wildfire activity in the western United States?, *Geophys. Res. Lett.*, *39*, L04703, doi:10.01029/02011GL050645.

Lean, J. (2000), Evolution of the Sun's spectral irradiance since the Maunder minimum, *Geophys. Res. Lett.*, *27*(16), 2425–2428, doi:10.1029/2000GL000043.

Linsley, B., H. Wu, E. Dassié, and D. Schrag (2015), Decadal changes in South Pacific sea surface temperatures and the relationship to the Pacific decadal oscillation and upper ocean heat content, *Geophys. Res. Lett.*, *42*, 2358–2366, doi:10.1002/2015GL063045.

MacDonald, G., and R. Case (2005), Variations in the Pacific Decadal Oscillation over the past millennium, *Geophys. Res. Lett.*, *32*, L08703, doi:10.01029/02005GL022478.

Mann, M., Z. Zhang, S. Rutherford, R. Bradley, M. Hughes, D. Shindell, C. Ammann, G. Faluvegi, and F. Ni (2009), Global signatures and dynamical origins of the Little Ice Age and Medieval Climate Anomaly, *Science*, *326*, 1256–1260, doi:10.1126/science.1177303.

Mantua, N., S. Hare, Y. Zhang, J. Wallace, and R. Francis (1997), A Pacific interdecadal climate oscillation with impacts on Salmon production, *Bull. Am. Meteorol. Soc.*, *78*, 1069–1079, doi:10.1175/1520-0477(1997)1078<1069:APICOW>1062.1060.CO;1062.

McCabe-Glynn, S., K. Johnson, C. Strong, M. Berkelhammer, A. Sinha, H. Cheng, and R. Edwards (2013), Variable North Pacific influence on drought in southwestern North America since AD 854, *Nat. Geosci.*, *6*, 617–621.

Minobe, S. (1997), A 50–70 year climatic oscillation over the North Pacific and North America, *Geophys. Res. Lett.*, *24*(6), 683–686, doi:10.1029/1097GL00504.

Moberly, R. (1968), Composition of magnesian calcites of algae and pelecypods by electron microprobe analysis, *Sedimentology*, *11*, 61–82.

Newman, M., et al. (2016), The Pacific Decadal Oscillation, revisited, *J. Clim.*, *29*, 4399–4427, doi:10.1175/JCLI-D-4315-0508.4391.

Nigam, S., M. Barlow, and E. Berbery (1999), Analysis links Pacific decadal variability to drought and streamflow in United States, *Eos Trans. AGU*, *80*(51), 621–625, doi:10.1029/1099EO00412.

Paillard, D., L. Labeyrie, and P. Yiou (1996), Macintosh program performs timeseries analysis, *Eos. Trans. AGU*, *77*, 379, doi:10.1029/1096EO00259.

Poli, P., H. Hersbach, P. Berrisford, D. Dee, A. Simmons, and P. Laloyaux (2015), ERA-20C Deterministic, Rep., 48 pp., Reading, U. K. [Available at www.ecmwf.int/sites/default/files/elibrary/2015/11700-era-11720c-deterministic.pdf.]

Rayner, N., D. Parker, E. Horton, C. Folland, L. Alexander, and D. Rowell (2003), Global analyses of sea surface temperature, sea ice, and night marine air temperature since the late nineteenth century, *J. Geophys. Res.*, *108*(D14), 4407, doi:10.1029/2002JD002670.

Reynolds, R., N. Rayner, T. Smith, D. Stokes, and W. Wang (2002), An improved in situ and satellite SST analysis for climate, *J. Clim.*, *15*, 1609–1625.

Rodionov, S., N. Bond, and J. Overland (2007), The Aleutian Low, storm tracks, and winter climate variability in the Bering Sea, *Deep Sea Res., Part II*, *54*, 2560–2577, doi:10.1175/JCLI3253.2561.

Salathe, E., Jr. (2006), Influences of a shift in North Pacific storm tracks on western North American precipitation under global warming, *Geophys. Res. Lett.*, *33*, L19820, doi:10.11029/12006GL026882.

Shakun, J. D., and J. Shaman (2009), Tropical origins of North and South Pacific decadal variability, *Geophys. Res. Lett.*, *36*, L19711, doi:10.1029/2009GL040313.

Simkin, T., and L. Siebert (1994), Volcanoes of the world, in *Global Volcanism Program*, 368 pp., Geoscience Press in association with the Smithsonian Institution, Tucson, Ariz. [Available at http://www.volcano.si.edu/world/.]

Smith, T., R. Reynolds, T. Peterson, and J. Lawrimore (2008), Improvements NOAAs Historical Merged Land–Ocean Temp Analysis (1880–2006), *J. Clim.*, *21*, 2283–2296, doi:10.1175/2007JCLI2100.2281.

Tierney, J., N. Abram, K. Anchukaitis, M. Evans, C. Giry, K. Kilbourne, C. Saenger, H. Wu, and J. Zinke (2015), Tropical sea surface temperatures for the past four centuries reconstructed from coral archives, *Paleoceanography*, *30*, 226–252, doi:10.1002/2014PA002717.

Torrence, C., and G. Compo (1998), A practical guide to wavelet analysis, *Bull. Am. Meteorol. Soc.*, *79*, 61–78.

Trenberth, K., and J. Hurrell (1994), Decadal atmosphere-ocean variations in the Pacific, *Clim. Dyn.*, *9*, 303–319, doi:10.1007/BF00204745.

Wang, S.-L., J. Huang, Y. He, and Y. Guan (2014), Combined effects of the Pacific Decadal Oscillation and El Niño-Southern Oscillation on global land dry–wet changes, *Nat. Sci. Rep.*, *4*, doi:10.1038/srep06651.

Williams, B., J. Halfar, K. DeLong, S. Hetzinger, R. Steneck, and D. Jacob (2014), Multi-specimen and multi-site calibration of Aleutian coralline algal Mg/Ca to climate signals, *Geochim. Cosmochim. Acta*, *139*, 190–204, doi:10.1016/j.gca.2014.1004.1006.

Worley, S., S. Woodruff, R. Reynolds, S. Lubker, and N. Lott (2005), ICOADS release 2.1 data and products, *Int. J. Climatol.*, *25*(7), 823–842, doi:10.1002/joc.1166.